

CEST of the Cervical Spinal Cord at 7 Tesla

Adrienne Dula¹, Siddharama Pawate¹, Lindsey M Dethrage¹, Benjamin N Conrad¹, Robert L Barry¹, and Seth A Smith¹
¹Vanderbilt University, Nashville, Tennessee, United States

PURPOSE: To use the increased frequency separation and signal to noise ratio in concert with prolonged T_1 at 7T to obtain signal enhancements necessary to detect subtle tissue changes in the spinal cord in healthy and multiple sclerosis (MS) subjects using chemical exchange saturation transfer (CEST) MRI.

METHODS: Optimal pulsed CEST saturation parameters (25-ms, $B_1 = 2 \mu\text{T}$) found via simulation were implemented for pulsed CEST MRI¹ in ten healthy controls and ten MS patients at 7T. Imaging used a multi-shot 3D gradient echo with multi-shot EPI (factor of 7), TR/TE/flip = 65 ms/7.2 ms/5°. The image in-plane resolution was $1.5 \times 1.6 \text{ mm}^2$ for five 5-mm slices using sensitivity encoding in both directions (factor = 2). Fat suppression was accomplished using a binomial excitation pulse resulting in a scan time of 5.46 s per image. Results were examined using traditional asymmetry analysis and Lorentzian fit method.

RESULTS: Distinct spectral features for all tissue types studied were found both up- and down-field from the water resonance with example data shown in Fig. 1. The z-spectra derived from all healthy subjects (Panel C, black) had the expected shape with CEST effects apparent from 2.0 ppm – 4.5 ppm and is compared to that derived from an MS lesion indicated by yellow arrows on the T_1 -w (A) and T_2 -w (B) images. This patient's normal appearing white matter (NAWM) and gray matter (GM) are shown in green and blue respectively and also demonstrate distinct differences compared to healthy control WM.

Average z-spectra from all subjects (Fig. 2, Panel A), including GM (blue line) normal appearing patient white matter (green line) and lesions (red line) demonstrated deviations in the MS population compared to healthy WM (black) indicating CEST's sensitivity to pathology. For all frequencies greater than +1 ppm, the Lorentzian difference (and z-spectra) for lesions and NAWM are distinct from healthy white matter (Panel B).

Pixel-wise histogram analyses of the Lorentzian difference were performed, Fig. 3, for the amide protons (3.5 ppm) in Panel A, as well as those resonances associated with the amine protons (3.0 ppm) in Panel B. At the amide resonance, the NAWM has an increased CEST effect while the lesions demonstrate a shoulder. At 3.0ppm, the histograms are more disperse for the NAWM whereas the lesions show no deviation from the healthy tissue.

DISCUSSION - It is apparent that the different tissue types exhibit distinct features at each resonance indicating the wealth of information obtained in the entire z-spectra. While all MS tissue types demonstrate CEST effects beginning around 1.5 ppm downfield from water, the NAWM has a wider range of deviations in saturation frequency offsets up to 4.5 ppm (Fig. 2). **CONCLUSION:** This study presents CEST imaging metrics that may be sensitive to the extensive and temporally varying biochemical neuropathology of MS in the spinal cord.

REFERENCES: 1. Jones CK, et al., MRM 2012;67(6):1579-1589.

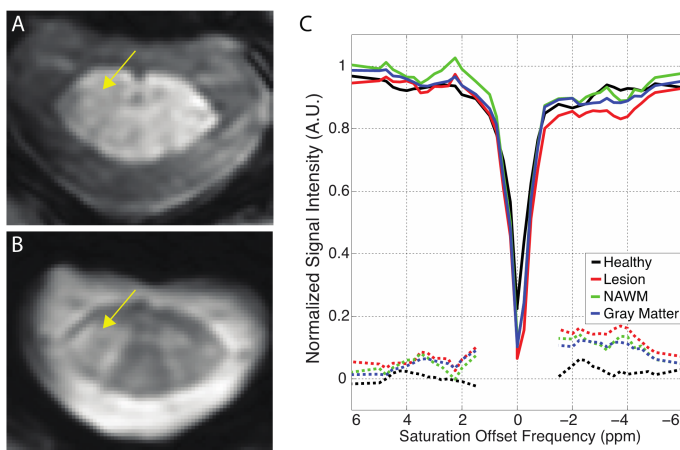


Figure 1 - Representative CEST data from a 40-year-old female patient with relapsing-remitting Multiple Sclerosis presenting with a lesion at the level of C2. A) T_1 -weighted axial slice and, B) T_2 -weighted axial slice with yellow arrows indicating lesion location C) z-spectrum from regions of interest encompassing the lesion (red, solid), normal appearing white matter (green, solid), and gray matter (blue, solid) are compared to that of the healthy subjects (black, solid). Additionally, the calculated Lorentzian differences are shown as dashed lines in the respective

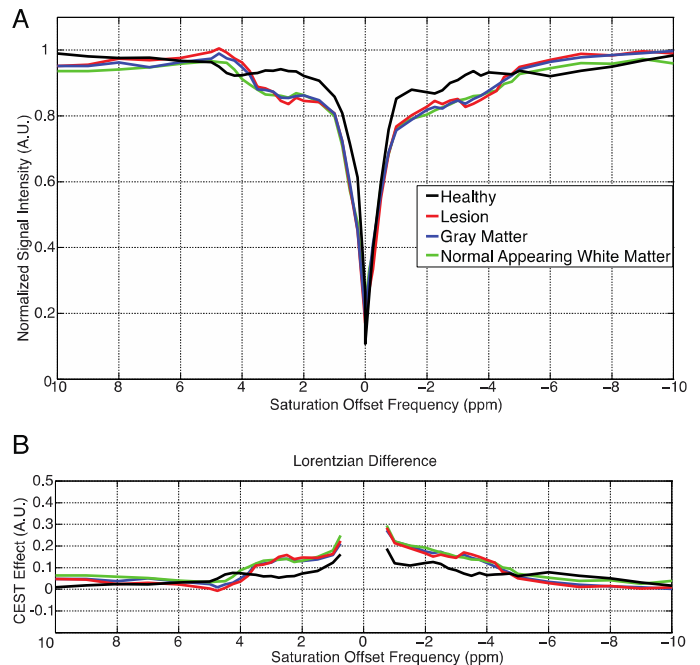


Figure 2 - Comprehensive results from all study participants. A) z-spectra from the spinal cord of healthy subjects at the level of C2/3 (black) and regions of interest from patients drawn to encompass lesion (red), normal appearing white matter (green), and gray matter (blue) showing the signal intensity as a function of saturation frequency offset. B) Quantification of the CEST effect calculated asymmetry, C) Quantification of the CEST effect calculated Lorentzian difference

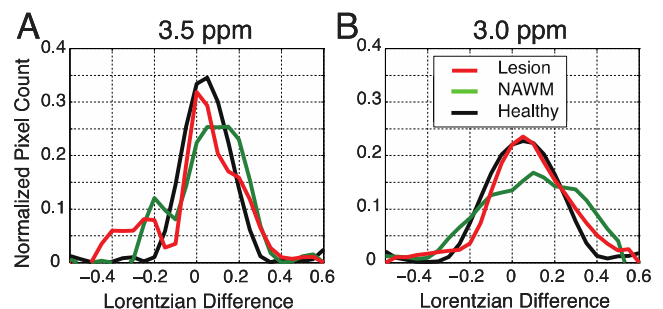


Figure 3 - Comprehensive data from all subjects depicting pixel-wise analysis of the CEST effect at the saturation frequency offsets of 3.5 ppm (A) and 3.0 ppm (B). Panels A&B display histograms of the calculated Lorentzian difference normalized by the total number of pixels for regions of interest in healthy tissue (black), lesion (red) and normal appearing white matter (green).